ORIGINAL ARTICLE

Biological Response to Nanostructure of Carbon Nanotube/titanium Composite Surfaces

Erika NISHIDA[1], Hirofumi MIYAJI[1], Junko UMEDA[2], Katsuyoshi KONDOH[2], Hiroko TAKITA[3], Izumi KANAYAMA[1], Saori TANAKA[1], Akihito KATO[1], Bunshi FUGETSU[4], Tsukasa AKASAKA[5], and Masamitsu KAWANAMI[1]

[1]Department of Periodontology and Endodontology, Hokkaido University Graduate School of Dental Medicine, Sapporo, Japan
[2]Joining and Welding Research Institute, Osaka University, Ibaraki, Japan
[3]Support Section for Education and Research, Hokkaido University Graduate School of Dental Medicine, Sapporo, Japan
[4]Nano-Agri Lab, Policy Alternatives Research Institute, The University of Tokyo, Tokyo, Japan.
[5] Department of Biomaterials and Bioengineering, Hokkaido University Graduate School of Dental Medicine, Sapporo, Japan

Synopsis
Titanium (Ti) is frequently used as a biomaterial in dental and orthopedic implants and in bone fixation devices. Effective modification of the Ti surface plays a crucial role in improving biocompatibility. Carbon nanotubes (CNTs) are among the most interesting nanomaterials due to their unique properties. In this study, we fabricated CNT-Ti composite surfaces by annealing Ti plates covered by different sized CNTs (Nanocyl NC 7000, 9.5 nm diameter and VGCF-H, 150 nm diameter). The properties of these surfaces were examined by scanning electron microscopy, X-ray diffraction, energy dispersive X-ray spectroscopy, raman spectroscopy, contact angle measurement and osteoblast-like cell seeding. In addition, samples were implanted into the subcutaneous tissue of rats. The three-dimensional nanostructures of CNTs and creation of titanium carbide were evident on the Ti surfaces, suggesting that the CNTs were well-anchored onto the Ti plates. CNT modification promoted desirable cell behavior, including cell spreading and proliferation, especially on the Nanocyl-modified surface. Inflammatory response was rarely observed on the Nanocyl surface, but macrophage-like giant cells were frequently observed on the VGCF-H surface. Therefore, the nanomorphology of narrow diameter CNTs provides a CNT-Ti composite surface with good biocompatibility.

Key words: *carbon nanotube, titanium, nanostructure, cell proliferation, biocompatibility*

Introduction

Titanium (Ti) is used in dental and orthopedic implants and in bone fixation devices [1-3] because of its strength and biological compatibility, including osseointegration. The surface characteristics of a Ti implant typically play a crucial role in the ability of the implant to adhere to soft and hard tissue. Different Ti surface- modification techniques, such as sandblasting [4], plasma-spraying [5], ceramic coating [6] and

acid-etching [7], have been investigated to improve the surface of Ti implants [8-9], but poor osseointegration and peri-implantitis remain problematic [10].

Recently, many research studies have shown that the fabrication of nanostructures on a biomaterial surface improves its biocompatibility [11, 12]. The introduction of nanostructures and nanopatterns enormously increases the surface area of the biomaterial, greatly increasing the wettability and protein absorption properties of the biomaterial [13]. In addition, nano- modified surfaces promote critical cellular actions such as cell proliferation and differentiation [14, 15]. Therefore, the introduction of well-controlled nanostructures on a Ti surface would enhance the self-assembly and self-organization processes required for successful implant adoption by the host.

Carbon-based nanomaterials have been extensively studied for biomedical applications. In particular, carbon nanotubes (CNTs) have novel and useful biological properties, and hold promise for use in biomedical devices as drug-delivery and tissue engineering scaffolds [16-19]. Morphological changes resulting from a CNTs coating have been shown to enhance the bioactivity of a three-dimensional scaffold [20]. CNTs provided new properties to a regenerative scaffold, including mechanical strength, biocompatibility, and enhanced cell activity and bone tissue deposition [21]. Akasaka *et al*. reported that CNTs effectively induced nucleation and growth of apatite crystallites [22]. Therefore, the biocompatibility of Ti implants could be enhanced by CNTs coating.

Several procedures for the nano- modification of Ti and Ti alloys using CNTs have been presented. For example, Terada *et al*. reported a CNT-collagen coating comprising a CNT layer laminated onto the surface of a collagen coating on the Ti; thus, the CNTs did not bind to the Ti surface directly [23]. Balani *et al*. demonstrated that hydroxyapatite -CNT coating onto Ti was performed by plasma spraying [24]. Furthermore, CNTs could be directly fixed onto a Ti surface through annealing. For example, Umeda *et al*. and Kondoh *et al*. reported that annealing of well-dispersed CNTs on a Ti surface generated a uniform CNT-Ti composite surface [25, 26]. This easy method, in which Ti surface is modified by coating and annealing of CNTs, may be widely selected for future clinical trials. We postulated that covering a Ti surface with CNT nanostructures by annealing would provide the biological properties required for biomedical applications. Accordingly, the aim of this study was to compare and assess the biological responses to a CNT-Ti composite surface and a pure Ti surface.

Materials and Methods

Fabrication of CNT-Ti composite surface

Two types of multi-walled CNTs were used: Nanocyl NC 7000 (9.5 nm diameter, Nanocyl, Sambreville, Belgium) and VGCF-H (150 nm diameter, Showa Denko, Tokyo, Japan). Each CNT was dispersed in an isopropyl alcohol-(IPA-) based zwitterionic surfactant solution at a concentration of 1 wt% as described previously [27]. A pure Ti plate (7 × 7 × 1 mm, purity: 99.5 %, The Nilaco Corporation, Tokyo, Japan) was dip-coated into each CNT dispersion. After drying, Ti plates were annealed at 850°C in a vacuum furnace to remove residual IPA solution, resulting in a thin CNT film on the Ti. The surface and cross section of each sample were characterized using a scanning electron microscopy (SEM, JSM-6500F, JEOL, Tokyo, Japan) coupled with an energy dispersive X-ray spectroscopy unit (EDS, JED-2300, JEOL) at 15 kV acceleration voltage. Changes in the nanostructures of Ti and the CNT layers were examined by X-ray diffraction (XRD, XRD-6100, Shimadzu, Kyoto, Japan) using Cu Kα radiation at 40 kV and 30 mA. Diffractograms were obtained from 2θ = 30° to 80° at 0.02° increments at a scanning speed of 2°/minute. Raman data were collected and analyses were conducted using a Raman spectrophotometer (LabRAM ARAMIS, Horiba, Kyoto, Japan) and associated software; a 532 nm laser was selected, and the acquisition time was 10 seconds. The hydrophilicity of the surface of each sample was investigated using a contact angle meter (DMs-200, Kyowa Electronic Instruments, Tokyo, Japan).

Cell morphology

Mouse osteoblastic MC3T3-E1 cells (1×10^4; RIKEN BioResource Center, Tsukuba, Japan) were seeded on Ti surfaces modified with Nanocyl or VGCF-H, and cultured in humidified 5% CO_2 at 37°C using medium (MEM alpha-GlutaMAX™-I; Thermo Fisher Scientific, Waltham, MA, USA) supplemented with 10% fetal bovine serum (FBS, Qualified; Thermo Fisher Scientific) and 1% antibiotics (penicillin/streptomycin; Thermo Fisher Scientific). A pure Ti plate without CNTs was used as a control. After 24 hours of culture, samples were fixed in 2.5% glutaraldehyde in 0.1 M sodium cacodylate
buffer (pH 7.4) for 30 min, rinsed in cacodylate buffer solution, and then dehydrated in increasing concentrations of ethanol. Following critical point drying, samples were analyzed using SEM (S-4000, Hitachi, Tokyo, Japan) at an acceleration voltage of 10 kV after coating with a thin layer of Pt-Pd.

Proliferation assay

MC3T3-E1 cells (1×10^5) were seeded on CNT-Ti composite surfaces and cultured in humidified 5% CO_2 at 37°C using a medium supplemented with 10% FBS and 1% antibiotics as above. A pure Ti plate without CNTs was used as a control. Cell viability was assessed after 2 and 7 days culture using a cell counting kit-8 (CCK-8, Dojindo Laboratories, Kumamoto, Japan) following the manufacturer's instructions. The optical density was measured using a microplate reader at an absorbance of 450 nm.

***In vivo* test**

The experimental protocol followed the institutional animal use and care regulations of Hokkaido University (Animal Research Committee of Hokkaido University, Approval No. 13-76). Eight 10-week-old male Wistar rats weighing 190 to 210 g were given general anesthesia by intraperitoneal injection of 0.6 mL / kg sodium pentobarbital (Somnopenthyl, Kyoritsu Seiyaku, Tokyo, Japan), as well as a local injection of 2% lidocaine hydrochloride with 1:80,000 epinephrine (Xylocaine Cartridge for Dental Use, Dentsply-Sankin K.K., Tokyo, Japan). After a skin incision was made, individual Ti plates were implanted into the subcutaneous tissue of the back of each rat. Skin flaps were sutured (Softretch 4-0, GC, Tokyo, Japan) and tetracycline hydrochloride ointment (Achromycin Ointment, POLA Pharma, Tokyo, Japan) was applied to the wound.

Rats were euthanized using an overdose of sodium pentobarbital (2 mL/kg) at 10 days post-surgery. Following removal of the Ti plate, tissue was excised and tissue blocks were fixed in 10% buffered formalin, embedded in paraffin wax, and cut into 6 μm sections. Sections were stained with hematoxylin-eosin (HE) and examined using light microscopy. The number of giant cells was assessed using three stained sections (200×): one from the center of the excised tissue sample, and one from tissue 1 mm to either side of the center.

In addition, Ti plate were removed at 35 days post-surgery and fixed in 10% buffered formalin and dehydrated in increasing concentrations of ethanol. Samples were analyzed using SEM (S-4000) at an acceleration voltage of 10 kV after coating with a thin layer of Pt-Pd.

Statistical analysis

The means and standard deviations of each parameter were calculated for each group. Statistical analysis was performed using the Scheffé test on each measurement. P-values < 0.05 were considered statistically significant. All statistical procedures were performed using a software package (IBM SPSS 11.0; IBM SPSS Japan, Tokyo, Japan).

Results

Characterization of CNT-Ti composite surface

Ti plates were discolored following coating and annealing with Nanocyl or VGCF-H (Figure 1A). SEM observations showed that a network of CNTs (CNT-net) was fabricated on the Ti surface and was composed of a three-dimensional reticulated CNT structure. CNTs had apparently disassembled into individual tubes. Nanocyl CNTs appeared to be slender and flexible in contrast to VGCF-H CNTs (Figure 1B, C).

XRD patterns for the CNT-Ti composite surfaces and pure Ti are shown in Figure 2. Titanium carbide (TiC) peaks associated with the

solid-phase Ti/carbon reaction were detected following annealing of the CNT covered plates, indicating that carbon atoms were dissolved into the Ti plate.

An EDS analysis of the CNT-Ti composite surface provided the Ti and carbon content (Table 1). The Ti surface treated with Nanocyl comprised approximately 42% elemental carbon, whereas the Ti surface treated with VGCF-H was approximately 73% carbon. The lower carbon content for the Nanocyl treated plates is due to the fact that these nanotubes have a much smaller diameter (9.5 nm) than VGCF-H nanotubes (150 nm), and so more easily form a dense film on the Ti plate surface. This leads to a more effective solid-state reaction with Ti, thus producing a thinner CNT film. SEM-EDS analysis of a cross section of a Ti plate coated with CNTs is shown in Figure 3, where the red line indicates the scan line, the green line shows the carbon content and the blue line shows the Ti content. For both specimens, a TiC layer was clearly detected at the interface between the Ti plate surface and the CNT film.

Raman spectroscopic analysis of each CNT-Ti composite surface showed peaks from the graphite structure-derived G-band and the defect-derived D-band around 1590 cm^{-1} and 1350 cm^{-1}, respectively. The G/D ratio for pre- and post-annealing was 0.89 to 0.87 for Nanocyl and 3.56 to 3.35 for VGCF-H. The essentially unchanged G/D ratio between pre- and post-annealing suggests that CNTs are not destroyed by heat treatment at high temperature (Figure 4).

The contact angle for the CNT-Ti composite surface was significantly higher than that for the pure Ti surface, with the VGCF CNT-net producing a significantly greater hydrophobic effect than Nanocyl (Figure 5).

Cell morphology

At 1 day of cell culture, SEM observation showed clearer cell spreading on the Nanocyl CNT-net than on the VGCF-H CNT-net or pure Ti plate (Figure 6). On Nanocyl, the cells were star-shaped with multiple elongated cytoplasmic protrusions (Figure 6A, G). It seemed likely that the cells used the CNT fibers as a scaffold and that cell attachment and spreading occurred preferentially on the CNT fibers. Although cells did attach to the VGCF CNT-net, they were generally thin and spindle-shaped, suggesting that the nanomorphology of this CNT-net was incompatible with vigorous cell growth and spreading (Figure 6B). Furthermore, cells were frequently penetrated by VGCF-H fibers in the CNT-net (Figure 6H). At 3 day, cell spreading was exhibited on VGCF-H CNT-net and Ti as well as Nanocyl CNT-net (Figure 6E, F). Marked cell growth was observed on the Nanocyl modified surface (Figure 6D).

Proliferation assay

The degree of cell proliferation on each sample is presented in Figure 6I. After 7 days, cell proliferation on both CNT-Ti composite surfaces was significantly greater than that the pure Ti surface, with the Nanocyl modified surface showing higher cell proliferation than the VGCF-H modified surface.

In vivo test

Histological observations 10 days after implantation into rat subcutaneous tissue showed minimal inflammatory cell infiltration in the connective tissues around the Nanocyl CNT-net and the pure Ti, suggesting that these samples possessed good biocompatibility (Figure 7A, C). However, aggregates of macrophage-like giant cells were observed on the surface of the VGCF-H modified surface (Figure 7B) to a much greater extent than on pure Ti and the Nanocyl modified surface (Figure 7D).

In SEM observation of the samples after 35 days, the CNT-net structure remained intact on the Ti surface. Cells and extracellular matrices had attached to the CNT-net surface. These observations suggest that the bonds between CNT-net and Ti are stable in the body (Figure 8).

Table 1 Elemental composition (at %) of CNT-Ti composite by EDS analysis.

	Ti	C
Nanocyl	58.0	42.0
VGCF-H	26.2	73.8

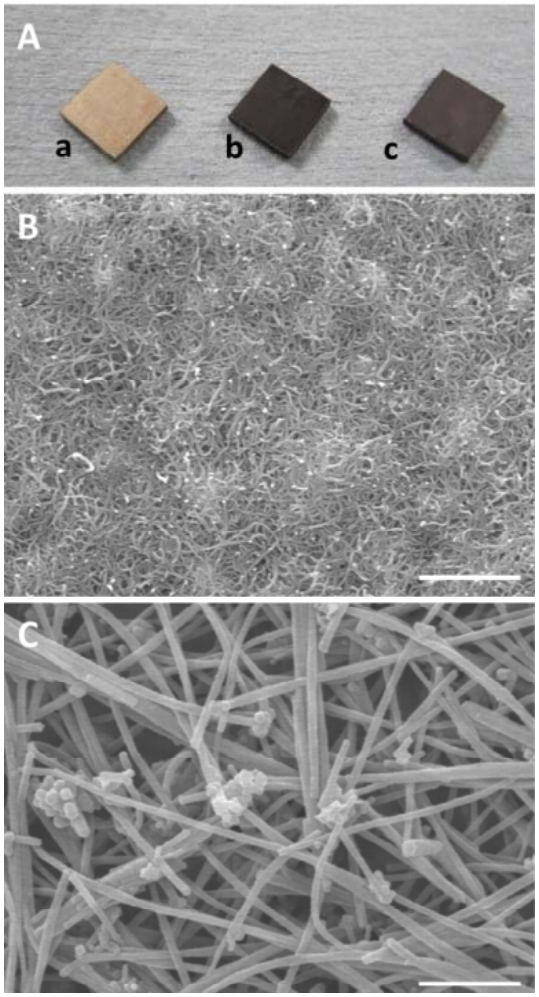

Figure 1
(A) CNT-Ti composite. (a) Pure Ti plate. (b) Ti plate coated with Nanocyl. (c)Ti plate coated with VGCF-H. (B) SEM image of a Nanocyl CNT-net. (C) SEM image of a VGCF CNT-net. Scale bars represent 1 µm (B, C).

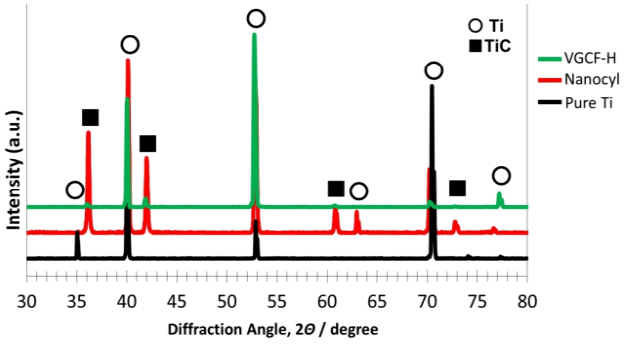

Figure 2
XRD patterns for pure Ti, Nanocyl CNT-net and VGCF CNT-net.

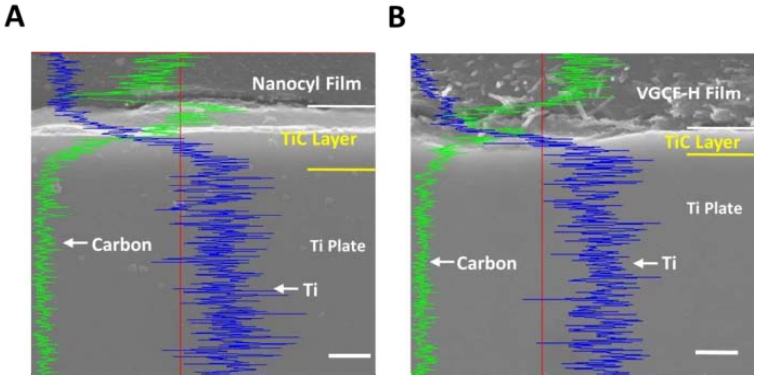

Figure 3
EDS analysis of a cross section of Ti treated with Nanocyl (A) and VGCF-H (B). Scale bars represent 1 µm.

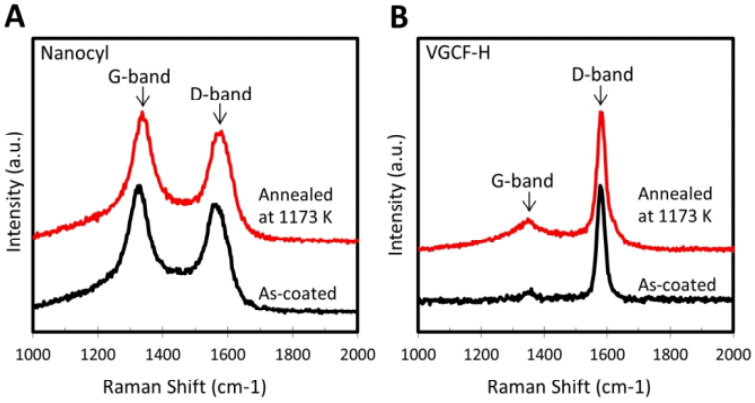

Figure 4
Raman spectra of Ti coated with Nanocyl (A) and VGCF-H (B).

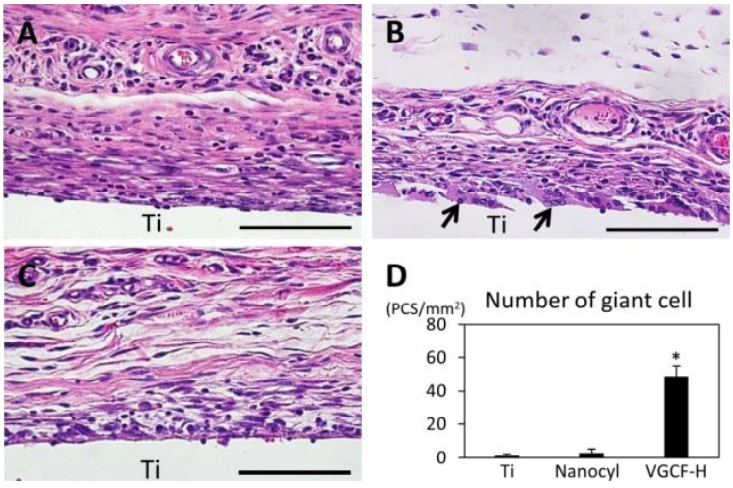

Figure 7
Histological findings at 10 days. (A) Nanocyl. (B) VGCF-H. (C) Pure Ti plate. Macrophage-like giant cells (arrows) were observed close to the VGCF-H surface. Scale bars represent 100 µm (A, B, C). Staining: hematoxylin and eosin. (D) Number of giant cells.

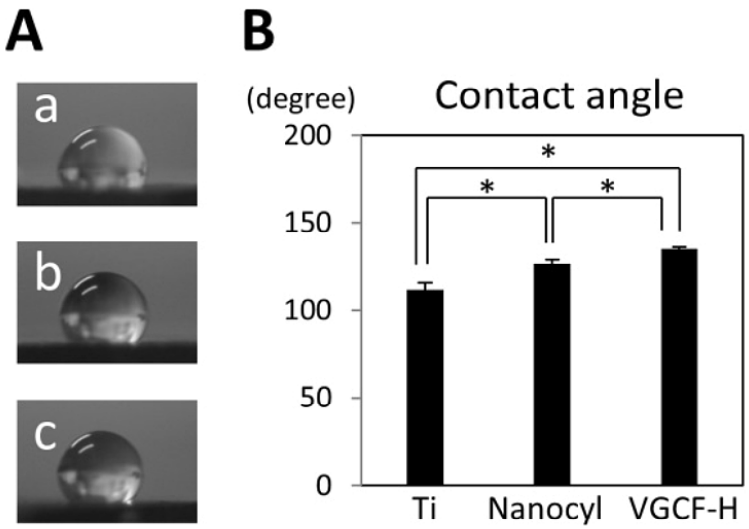

Figure 5
(A) Contact angle images. (a) Pure Ti plate. (b) Ti plate coated with Nanocyl. (c)Ti plate coated with VGCF-H. (B) Bar graph summarizing the contact angle data.

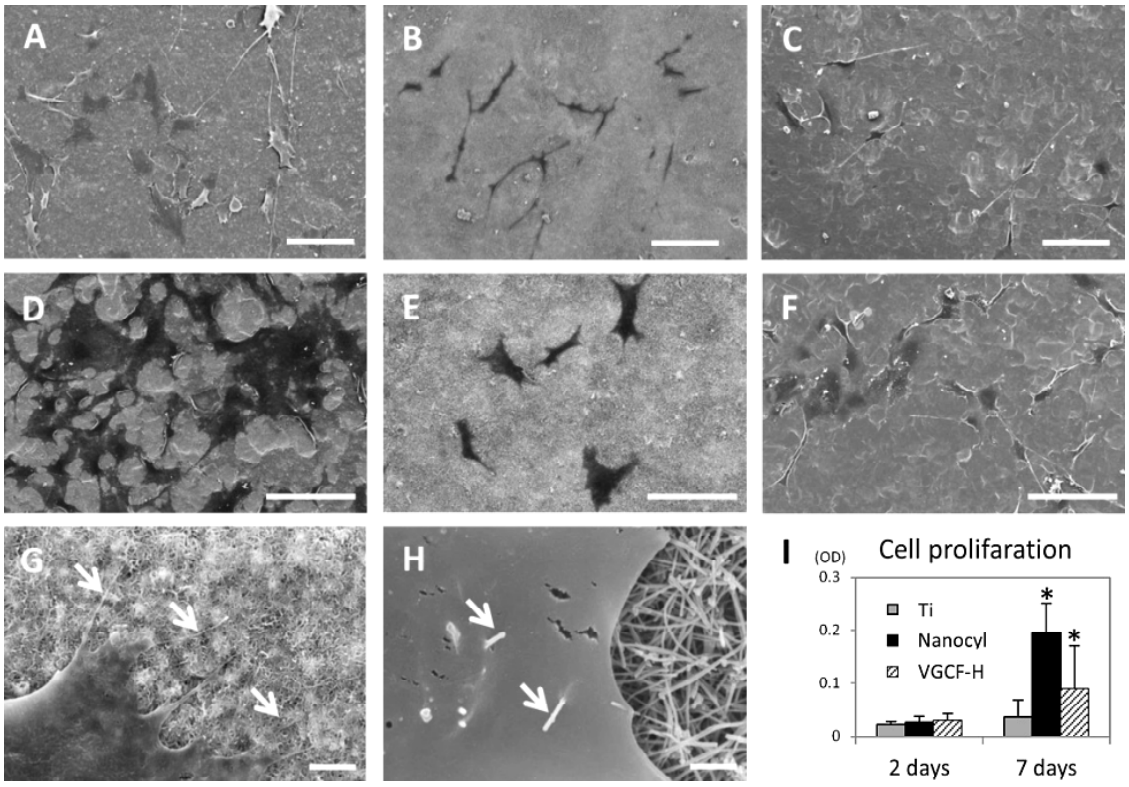

Figure 6
(A) SEM micrograph showing cell morphology on Nanocyl at 1 day. Cells were widely distributed on the Nanocyl CNT-net. (B) SEM micrograph showing cell morphology on VGCF-H at 1 day. The cells appeared to be spindle shaped. (C) SEM micrograph showing cell morphology on pure Ti at 1 day. (D) SEM micrograph showing cell morphology on Nanocyl at 3 days. Cells was proliferated on Nanocyl net. (E) SEM micrograph showing cell morphology on VGCF-H at 3 days. Cell spreading was likely occurred on the VGCF-net. (F) SEM micrograph showing cell morphology on pure Ti at 3 days. (G) Higher magnification of panel A. Cytoplasmic protrusions were frequently observed on Nanocyl CNT-net (arrows). (H) Higher magnification of panel B. VGCF-H fibers pierced the cells (arrows). Scale bars represent 100 μm (A, B, C, D, E, F), 2 μm (G) and 1μm (H). (I) In vitro assessment of cell proliferation using the CCK-8 assay.

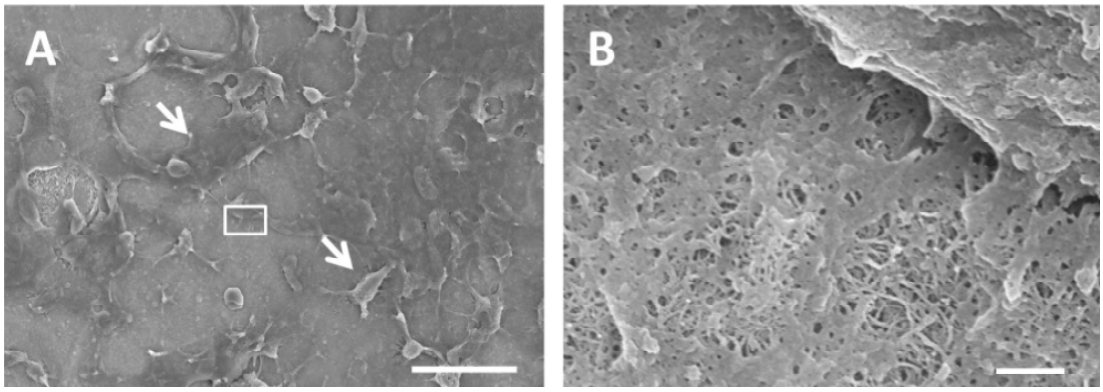

Figure 8
(A) SEM micrograph of Ti plate coated with Nanocyl retrieved from rat subcutaneous tissue showing cells attached (arrows) to the CNT-net. (B) Higher magnification of the framed area in panel A. The nano-structure of the CNT-net can be observed. Scale bars represent 20 μm (A) and 500 nm (B).

Discussion

SEM observation showed significant cell spreading on Nanocyl-net (Figure 6), with a particularly well-formed cell pseudopodial network, suggesting that the nanomorphology of the Nanocyl modified surface improved the cytocompatibility of Ti. Several earlier reports indicated that cells spread on a CNT layer, using it as a scaffold; for example, adhesion of cultured cells was increased by a CNT-net coating, thus providing a regenerative scaffold [28]. However, in the present study, the VGCF-H CNT-net resulted in spindle shaped cells, suggesting that the biocompatibility of the VGCF-H nanostructure was lower than that for Nanocyl, and that cells could recognize the differences in morphology between Nanocyl and VGCF CNT-nets. In general, cells well-attach to relevant hydrophobic surfaces via their cell membrane [29, 30]. We found that the VGCF-H surface was more hydrophobic than the Nanocyl surface (Figure 5). It was suggested that both the nanostructure and the hydrophilicity of the CNT-Ti composite surface significantly influenced cell morphology and behavior.

Osteoblast cell proliferation was stimulated more by CNT modified surfaces than by a pure Ti surface (Figure 6I). Nano-modification of a biomaterial surface may result in morphological changes to the surface, such as increased roughness and surface area, thereby enhancing cell attachment and adsorption of signaling molecules [31, 32]. Similarly, Watari *et al*. and Yao *et al*. reported that nano-modification of a material surface promoted bone cell proliferation [33, 34]. Thus, CNT nanomodification seems to confer novel properties to the Ti surface. In addition, the Nanocyl surface promoted cell proliferation significantly more than the VGCF-H surface. Recently, many studies have demonstrated an association between the size of CNTs and their biological effects. Von der Mark *et al*. demonstrated that 15 nm diameter TiO_2 nanotubes enhanced cell attachment and proliferation more than 100 nm nanotubes, and the larger TiO_2 nanotubes increased cell apoptosis [32]. Furthermore, SEM images frequently showed cells were pierced by VGCF-H nanotubes (Figure 6H). Yamashita *et al*. demonstrated that long, thick CNTs, but not short, thin CNTs, caused significant DNA damage and inflammatory response [35]. The Nanocyl nanotubes used in this experiment were 9.5 nm in diameter and 1.5 μm in length, whereas the VGCF-H nanotubes were 150 nm in diameter and 15 μm in length. Accordingly, Nanocyl would be expected to exhibit superior flexibility compared to VGCF-H and provide a non-cytotoxic, biocompatible CNT-Ti composite surface. Further studies are required to assess the relation between osseointegration and size of CNTs in bone tissue.

Annealing and electrophoretic deposition was found to bind CNTs strongly and directly to the Ti surface [36, 37], preventing CNT detachment during implantation. Annealing of a well-dispersed CNT solution produced a thin,

uniform CNT film with a network-like structure [25, 26]. In addition, the XRD results clearly showed that annealing resulted in the formation of TiC (Figure 2), indicating that CNTs partially dissolved into the Ti plate, thereby strongly binding the CNTs to the Ti surface. TiC is a biosafe material with good biocompatibility [38, 39]. It is possible that the thickness of the CNT layer can be regulated by the annealing time and temperature. Further studies are needed to identify the optimal CNT annealing conditions for biomedical applications.

The results of the *in vivo* test showed few inflammatory cells on the Nanocyl surface, but many macrophage-like giant cells were detected on the VGCF-H surface (Figure 7), suggesting that differences in CNT nanomorphology influenced cell behavior and tissue response both *in vivo* and *in vitro*. Several studies reported the accumulation of blackened macrophage-like cells on a CNT substrate, indicative of phagocytosis [28]; however, this was not observed with the Nanocyl samples. Champion *et al*. reported that particle size of foreign body strongly affected the phagocytosis and attachment of macrophages [40]. They exhibited that microspheres with 2-3 μm sizes were phagocytosed more readily than smaller particles. Therefore, it seemed likely that macrophage-like cells recognized the submicron VGCF-H network structure, whereas inflammatory cells could not recognize and respond to the Nanocyl nano-sized network. In addition, detachment of CNTs from the Ti surface may result in free CNTs adversely affecting the body. Sato *et al*. investigated the structure of 15 nm diameter CNTs following implantation for 2 years in the subcutaneous tissue of rats and observed that the CNTs were gradually degraded inside macrophage lysosomes. None of the rats displayed symptoms of cancer or severe inflammatory reactions, including necrosis [41]. The long-term effects of *in vivo* CNT use should be further evaluated prior to future clinical trials.

Conclusion

We fabricated CNT-Ti composite surfaces by annealing Ti plates covered with CNTs and investigated the biological response to CNT nanomorphologies. CNT-Ti composite surfaces promoted desirable cell behavior, including cell proliferation, compared with pure Ti. Furthermore, nanomodification with CNTs, particularly with narrow diameter Nanocyl, provided good biocompatibility.

Acknowledgements

This work was supported by The Akiyama Life Science Foundation and JPSP KAKENHI Grant Number 25463210. This work was performed under the cooperative research program of Joining and Welding Research Institute, Osaka University. The authors report no conflicts of interest related to this study.

References

1) Sinha RK, Tuan RS. Regulation of Human osteoblast integrin expression by orthopedic implant materials. Bone 1996;18:451-457.
2) Bathomarco RV, Solorzano G, Elias CN, Prioli R. Atomic force microscopy analysis of different surface treatments of Ti dental implant surfaces. Applied Surface Science 2004;233: 29-34.
3) Liu X, Chu PK, Ding C. Surface modification of titanium, titanium alloys, and related materials for biomedical applications. Mater Sci Eng A 2004;R 47:49-121
4) Anselme K, Bigerelle M. Topography effects of pure titanium substrates on human osteoblast long-term adhesion. Acta Biomater 2005;1:211-222
5) Si J, Zhang J, Liu S, Zhang W, Yu D, Wang X, Guo L, Shen SG. Characterization of a micro-roughened TiO2/ZrO2 coating: mechanical properties and HBMSC responses in vitro. Acta Biochim Biophys Sin 2014;46:572-581.
6) Nakashima Y, Hayashi K, Inadome T, Uenoyama K, Hara T, Kanemaru T, Sugioka Y, Noda I. Hydroxyapatite-coating on titanium arc sprayed titanium implants. J Biomed Mater Res 1997;35:287-298.
7) Gahlert M, Röhling S, Wieland M, Sprecher CM, Kniha H, Milz S. Osseointegration of zirconia and titanium dental implants: a histological and histomorphometrical study in the maxilla of pigs. Clin Oral Implants Res 2009;20:1247-1253.
8) Jones FH. Teeth and bones: applications of surface science to dental materials and related biomaterials. Surf Sci Report 2001;42:75-205.
9) Li LH, Kong YM, Kim HW, Kim YW, Kim HE, SJ Heo, Koak JY. Improved biological performance of Ti implants due to surface modification by micro-arc oxidation. Biomaterials 2004;25:2867-2875.
10) Koka S, Zarb G. On osseointegration: the healing adaptation principle in the context of

osseosufficiency, osseoseparation, and dental implant failure. Int J Prosthodont 2012;25:48-52.
11) Yang Y, Kim KH, Ong JL. A review on calcium phosphate coatings produced using a sputtering process —an alternative to plasma spraying. Biomaterials 2005;26:327-337.
12) Kwok CT, Wong PK, Cheng FT, Man HC. Characterization and corrosion behavior of hydroxyapatite coatings on Ti6Al4V fabricated by electrophoretic deposition. Applied Surface Science 2009;255:6736-6744.
13) Woo KM, Chen VJ, Ma PX. Nano-fibrous scaffolding architecture selectively enhances protein adsorption contributing to cell attachment. J Biomed Mater Res A 2003;67:531-537.
14) Kalita SJ, Bhardwaj A, Bhatt HA. Nanocrystalline calcium phosphate ceramics in biomedical engineering. Mater Sci Eng C 2007; 27:441-449.
15) Ibara A, Miyaji H, Fugetsu B, Nishida E, Takita H, Tanaka S, Sugaya T, Kawanami M. Osteoconductivity and biodegradability of collagen scaffold coated with nano-β-TCP and fibroblast growth factor 2. J Nanomater 2013; 46:1-11.
16) Liu Z, Tabakman S, Welsher K, Dai H. Carbon Nanotubes in Biology and Medicine: In vitro and in vivo detection, imaging and drug delivery. Nano Res 2009;2:85-120.
17) Usui Y, Aoki K, Narita N, Murakami N, Nakamura I, Nakamura K, Ishigaki N, Yamazaki H, Horiuchi H, Kato H, Taruta S, Kim YA, Endo M, Saito N. Carbon nanotubes with high bone-tissue compatibility and bone-formation acceleration effects. Small 2008;4:240-246.
18) Tran PA, Zhang L, Webster TJ. Carbon nanofibers and carbon nanotubes in regenerative medicine. Adv Drug Deliv Rev 2009;61:1097-1114.
19) Dorj B, Won JE, Kim JH, Choi SJ, Shin US, Kim HW. Robocasting nanocomposite scaffolds of poly(caprolactone) / hydroxyapatite incorporating modified carbon nanotubes for hard tissue reconstruction. J Biomed Mater Res A.2013;101:1670-1681.
20) Hirata E, Uo M, Nodasaka Y, Takita H, Ushijima N, Akasaka T, Watari F, Yokoyama A. 3D collagen scaffolds coated with multiwalled carbon nanotubes:Initial cell attachment to internal surface. J Biomed Mater Res B Appl Biomater 2010;93:544-550.
21) Martins-Júnior PA, Alcântara CE, Resende RR, Ferreira AJ. Carbon nanotubes: directions and perspectives in oral regenerative medicine. J Dent Res 2013;92:575-583.
22) Akasaka T, Watari F, Sato Y, Tohji K. Apatite formation on carbon nanotubes. Mater Sci Eng C 2006;26:675-678.
23) Terada M, Abe S, Akasaka T, Uo M, Kitagawa Y, Watari F. Development of a multiwalled carbon nanotube coated collagen dish. Dent Mater J 2009;28:82-88.
24) Balani K, Anderson R, Laha T, Andara M, Tercero J, Crumpler E, Agarwal A. Plasma-sprayed carbon nanotube reinforced hydroxyapatite coatings and their interaction with human osteoblasts in vitro. Biomaterials 2007;28:618-624.
25) Umeda J, Mimoto T, Kondoh K, Fugetsu B. Wear behavior of network-structured carbon nanotube coating on titanium substrate. Transactions of JWRI 2012;41:49-52.
26) Kondoh K, Threrujirapapong T, Umeda J, Fugetsu B. High-temperature properties of extruded titanium composites fabricated from carbon nanotubes coated titanium powder by spark plasma sintering and hot extrusion. Compos Sci Technol 2012;72:1291-1297.
27) Fugetsu B, Han W, Endo N, Kamiya Y, Okuhara T. Disassembling single-walled carbon nanotube bundles by dipole / dipole electrostatic interactions. Chem Lett 2005;34: 1218-1219.
28) Hirata E, M´enard-Moyon C, Venturelli E, Takita H, Watari F, Bianco A, Yokoyama A. Carbon nanotubes functionalized with fibroblast growth factor accelerate proliferation of bone marrow-derived stromal cells and bone formation. Nanotechnology 2013;24:435101.
29) Kushida A, Yamato M, Konno C, Kikuchi A, Sakurai Y, Okano T. Temperature-responsive culture dishes allow nonenzymatic harvest of differentiated Madin-Darby canine kidney. J Biomed Mater Res A 2000;51:216-223.
30) McAuslan BR, Johnson G. Cell responses to biomaterials I: Adhesion and growth of vascular endothelial cells on poly(hydroxyethyl methacrylate) following surface modification by hydrolytic etching (MDCK) cell sheets. J Biomed Mater Res A 1987;21:921-935.
31) Yang F, Murugan R, Ramakrishna S, Wang X, Ma YX, Wang S. Fabrication of nano-structured porous PLLA scaffold intended for nerve tissue engineering. Biomaterials 2004;25:1891-1900.
32) von der Mark K, Park J, Bauer S, Schmuki P. Nanoscale engineering of biomimetic surfaces: cues from the extracellular matrix. Cell Tissue Res 2010;339:131-153.
33) Watari F, Takashi N, Yokoyama A, Uo M, Akasaka T, Sato Y, Abe S, Totsuka Y, Tohji K. Material nanosizing effect on living organisms: nonspecific, biointeractive, physical size effects. J R Soc Interface 2009;6:S371-388.
34) Yao C, Webster TJ. Anodization: a promising nano-modification technique of titanium implants for orthopedic applications. J Nanosci Nanotechnol 2006;6:2682-2692.

35) Yamashita K, Yoshioka Y, Higashisaka K, Morishita Y, Yoshida T, Fujimura M, Kayamuro H, Nabeshi H, Yamashita T, Nagano K, Abe Y, Kamada H, Kawai Y, Mayumi T, Yoshikawa T, Itoh N, Tsunoda S, Tsutsumi Y. Carbon nanotubes elicit DNA damage and inflammatory response rlative to teir sze and shape. Inflammation 2010;33:276-280.
36) Thomas BJC, Boccaccini AR, Shaffer MSP. Multi-wlled crbon nanotube coatings using electrophoretic deposition (EPD). J Am Ceram Soc 2005;88:980-982.
37) Patel KD, Kim TH, Lee EJ, Han CM, Lee JY, Singh RK, Kim HW. Nanostructured biointerfacing of metals with carbon nanotube / chitosan hybrids by electrodeposition for cell stimulation and therapeutics delivery. ACS Appl Mater Interfaces 2014:25325144
38) Jones MI, McColl IR, Grant DM, Parker KG, Parker TL. Protein adsorption and platelet attachment and activation, on TiN, TiC, and DLC coatings on titanium for cardiovascular applications. J Biomed Mater Res A 2000; 52: 413-421.
39) Cheng HC, Chiou SY, Liu CM, Lin MH, Chen CC, Ou KL. Effect of plasma energy on enhancing biocompatibility and hemocompatibility of diamond-like carbon film with various titanium concentrations. J Alloys Compd 2009;477:931-935.
40) Champion JA, Walker A, Mitragotri S. Role of particle size in phagocytosis of polymeric microspheres. Pharm Res 2008;25:1815-1821.
41) Sato Y, Yokoyama A, Nodasaka Y, Kohgo T, Motomiya K, Matsumoto H, Nakazawa E, Numata T, Zhang M, Yudasaka M, Hara H, Araki R, Tsukamoto O, Saito H, Kamino T, Watari F, Tohji K. Long-term biopersistence of tangled oxidized carbon nanotubes inside and outside macrophages in rat subcutaneous tissue. Sci Rep 2013;3:2516.

(Received: June 20, 2015/
Accepted: June 27, 2015)

Corresponding author*:*
Hirofumi Miyaji, D.D.S., Ph.D.
Department of Periodontology and Endodontology, Hokkaido University
Graduate School of Dental Medicine,
N13 W7 Kita-ku, Sapporo 060-8586, Japan
Tel: +81-11-706-4266, Fax: +81-11-706-4334
E-mail: miyaji@den.hokudai.ac.jp